medRxiv preprint doi: https://doi.org/10.1101/2023.03.03.23286579; this version posted March 6, 2023. The copyright holder for this preprint (which was not certified by peer review) is the author/funder, who has granted medRxiv a license to display the preprint in perpetuity. It is made available under a CC-BY-ND 4.0 International license .

What has brain diffusion MRI taught us on chronic pain: a critical review

Monica Sean[1,3 #], Graham Little[6 #], Paul Bautin[1,3], Marylie Martel[3], Maxime Descoteaux[6], Guillaume Léonard[4,5], Pascal Tétreault*[1,2,3]

1.Department of Anesthesiology, Faculty of medicine and health sciences, Université de Sherbrooke, Sherbrooke, Quebec, Canada
2.Department of Nuclear medicine and radiobiology, Faculty of medicine and health sciences, Université de Sherbrooke, Sherbrooke, Quebec, Canada
3.Centre de recherche du Centre hospitalier universitaire de Sherbrooke, Sherbrooke, Quebec, Canada
4. School of rehabilitation, Faculty of medicine and health sciences, Université de Sherbrooke, Sherbrooke, Quebec, Canada
5. Research Centre on Aging du Centre intégré universitaire de santé et de services sociaux de l'Estrie – Centre hospitalier universitaire de Sherbrooke, Sherbrooke, Quebec, Canada
6. Sherbrooke Connectivity Imaging Lab (SCIL), Computer Science Department, Université de Sherbrooke, Sherbrooke, Quebec, Canada
* Corresponding author: pascal.tetreault@usherbrooke.ca
# co-first authors

Keywords: brain, chronic pain, Magnetic Resonance Imaging (MRI), diffusion MRI, white matter

Running title: Diffusion MRI of the Brain in Chronic Pain

NOTE: This preprint reports new research that has not been certified by peer review and should not be used to guide clinical practice.

medRxiv preprint doi: https://doi.org/10.1101/2023.03.03.23286579; this version posted March 6, 2023. The copyright holder for this preprint (which was not certified by peer review) is the author/funder, who has granted medRxiv a license to display the preprint in perpetuity. It is made available under a CC-BY-ND 4.0 International license .

Abstract

Chronic pain is a widespread health condition affecting millions of individuals worldwide. Despite its high prevalence, the underlying neural mechanisms and pathophysiology of chronic pain are still not well understood. Introduced about 35 years ago, brain diffusion MRI has emerged as a powerful tool to investigate white matter microstructure and connectivity changes in chronic pain conditions. In this review, we provide an overview of the current state of research on brain diffusion MRI in chronic pain, including the methods used to acquire and analyze diffusion MRI data, as well as the major findings in the field.

We discuss the evidence supporting the role of altered white matter microstructure and connectivity in chronic pain conditions, highlighting the importance of studying multiple chronic pain syndromes to identify common neurobiological pathways. We also explore the potential clinical applications of diffusion MRI in chronic pain research, such as identifying biomarkers for diagnosis and treatment response.

In addition, we explore the shortcomings and difficulties associated with brain diffusion MRI in chronic pain studies, such as the necessity for uniformity in data acquisition and analysis methods. Finally, we discuss emerging techniques and future directions in brain diffusion MRI research that may provide new insights into the pathophysiology of chronic pain and potential new therapeutic targets. In summary, we are optimistic that brain diffusion MRI has significant potential in furthering our knowledge of chronic pain and enhancing clinical outcomes, although further research is required due to the limited body of literature currently available, and that targeted therapeutic strategies are yet to be identified.

medRxiv preprint doi: https://doi.org/10.1101/2023.03.03.23286579; this version posted March 6, 2023. The copyright holder for this preprint (which was not certified by peer review) is the author/funder, who has granted medRxiv a license to display the preprint in perpetuity. It is made available under a CC-BY-ND 4.0 International license .

Introduction

The understanding of chronic pain (CP) has greatly advanced over the past 25 years, with many scientists recognizing the significant role of brain processes in its development (1). A vast number of studies have now thoroughly documented the impact of various CP conditions on brain structure and function (2). When assessed using structural Magnetic Resonance Imaging (MRI) techniques, such as T1 or T2 weighted images, some brain impairments were found to be common across different pain conditions, such as reduced gray matter density (GMD) in the hippocampus and secondary somatosensory cortex. However, others were unique to specific types of CP, such as decreased GMD in the posterior insula in low back pain (LBP) compared to decreased GMD in the anterior insula in chronic regional pain syndrome (3). These studies have led to the unexpected identification of brain regions involved in chronic pain, including areas responsible for emotional learning, memory, and decision-making, rather than just the anticipated somatosensory regions. These changes may play a role in both the development and maintenance of CP, as seen in individuals transitioning to chronic low back pain (CLBP), who present smaller amygdala and hippocampi volumes (4).

Functional MRI (fMRI) studies have also indicated that regions outside of the somatosensory areas are largely involved in chronic pain. Areas known for processing cognitive, learning, and emotional information are found to have increased activity during the transition from acute to chronic pain (5). Chronic pain has also been shown to affect the organization of the brain at the network level. When studying resting state networks in various chronic pain conditions, research has found that the default mode network is the primary network undergoing reorganization due to an increase in sustained pain signaling through the medial prefrontal cortex (6). Some functional features are also capable of forecasting transition from a subacute phase to a chronic pain phase (7). Interestingly, these properties appear to be plastic and may partially reverse and reorganize upon receiving treatment or during the progression of the condition (8–10).

However, despite the tremendous progress made in MRI technology and analysis methods, the structural changes in white matter (WM) related to CP have been studied to a lesser extent. White matter is a highly complex system that makes up over one-third of the brain's

medRxiv preprint doi: https://doi.org/10.1101/2023.03.03.23286579; this version posted March 6, 2023. The copyright holder for this preprint (which was not certified by peer review) is the author/funder, who has granted medRxiv a license to display the preprint in perpetuity. It is made available under a CC-BY-ND 4.0 International license .

total volume and recent research has shown that various acute and chronic neurological conditions, such as Alzheimer's, Parkinson's, depression, multiple sclerosis, traumatic brain injury, and others, can affect the microstructure of white matter (11–16). Currently, diffusion-weighted MRI (DWI) is the most promising non-invasive tool for investigating WM structural changes. Although dMRI methods have advanced significantly in recent years (17), one of the earliest and still commonly used methods is to model the dMRI signal using diffusion tensor imaging (DTI). Accordingly, fractional anisotropy (FA), a common DTI measure, is one of the most widely reported dMRI measures to evaluate WM integrity. As most other fields, the pain research community is searching for valid biomarkers to help people suffering from this condition. For CP, we are searching for biomarkers that can predict the transition from acute to chronic pain and identify treatment response potential, and brain imaging is considered one of the most valid approaches (18–23). However, biomarkers from diffusion MRI for CP are currently under-investigated, but they hold promise for rapid clinical application (24–28). It is likely that CP biomarkers will soon be discovered using diffusion MRI due to the critical role that the brain plays in CP and its treatment.

The purpose of this review is to critically evaluate the current research on the characteristics of brain white matter as revealed through diffusion MRI methods and its impairments in various chronic pain conditions. We have used the latest definition of chronic pain provided by the International Association for the Study of Pain and its subcategories to classify the types of chronic pain (29,30). The focus was on chronic primary pain, which encompasses five categories: 1) chronic widespread pain, 2) complex regional pain syndrome, 3) chronic primary headache or orofacial pain, 4) chronic primary visceral pain, and 5) chronic primary musculoskeletal pain. After reviewing 447 publications, only 59 met the criteria, with the highest number of articles in category 3 (21 articles), and only two articles in category 2.

medRxiv preprint doi: https://doi.org/10.1101/2023.03.03.23286579; this version posted March 6, 2023. The copyright holder for this preprint (which was not certified by peer review) is the author/funder, who has granted medRxiv a license to display the preprint in perpetuity. It is made available under a CC-BY-ND 4.0 International license .

Methods

Information source

PubMed and Scopus databases were searched for articles dated up to 10th March 2022 Articles were also searched using the Medical Subject Headings (MeSH) term on PubMed.

Review strategy

This review follows the recommendations from the Preferred Reporting Items for Systematic reviews and Meta-Analyses extension for Scoping Reviews (PRISMA-ScR) Checklist. Search strategies were developed with a librarian of the Health Sciences Library of the Université de Sherbrooke. The keywords chosen for the review were: magnetic resonance imaging, diffusion, pain, and brain. The full search strategy can be viewed in the *supplementary material*.

Study strategy and inclusion/exclusion criterias

The study strategy is illustrated in Figure 1. First, we screened 447 articles to exclude review articles and articles that were ineligible based on the title and abstract (i.e., articles that did not contain the words "diffusion," "brain," or "pain,") . Second, we excluded case reports, articles not in English, and articles where pain was not the main focus. Third, we excluded studies that did not acquire dMRI in brain regions of individuals with chronic pain and studies that included participants who were under the age of one, veterans, amputees, or had undergone deep brain stimulation (DBS), traumatic brain injury (TBI), surgery, chronic pain from a stroke or neurodegenerative disease, or experimental acute pain. Methodological articles and animal studies were also excluded. Fourth, among the remaining articles, we separated them into three categories: chronic primary pain, chronic secondary pain based on the IASP classification (29,30), or articles missing information about the chronic pain condition, and only included articles on chronic primary pain. Finally, articles were excluded if dMRI analysis was done only on a nerve, only on healthy controls, or if no results were documented. One article was added after further investigation, as it was mentioned in several of the included articles and was found to have used dMRI in chronic pain patients but did not used our search terms in either the title or the abstract. The remaining articles were analyzed.

medRxiv preprint doi: https://doi.org/10.1101/2023.03.03.23286579; this version posted March 6, 2023. The copyright holder for this preprint (which was not certified by peer review) is the author/funder, who has granted medRxiv a license to display the preprint in perpetuity. It is made available under a CC-BY-ND 4.0 International license .

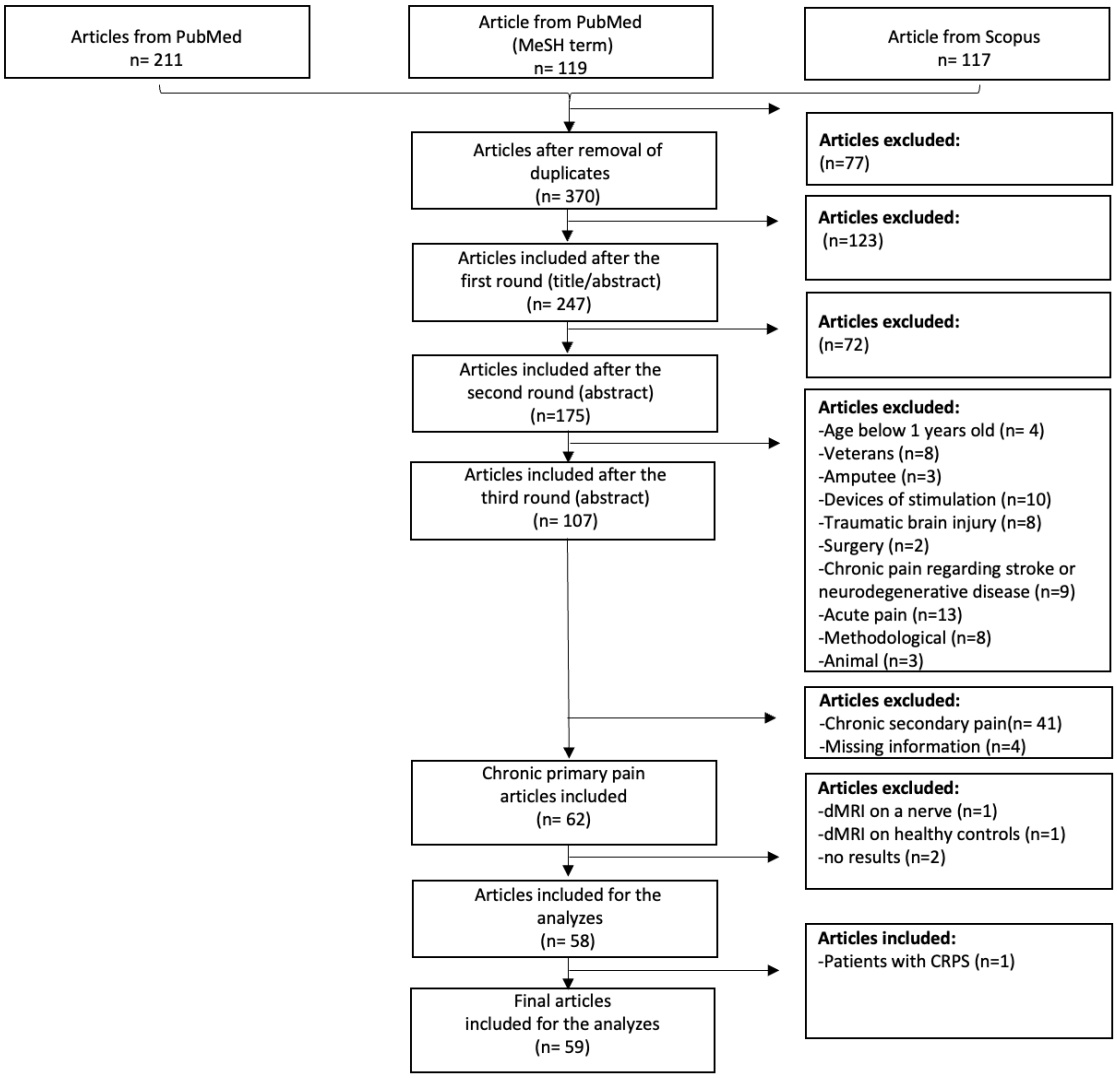

Figure 1. Flowchart for selection of articles to be included in the review.

Study selection and analyzes

The first three steps described in the section study strategy and inclusion and exclusion criteria were conducted by MS and PT. Any disagreement was resolved between MS and PT. Subsequently, the classification into primary chronic pain and secondary chronic pain was made by MS and supported by PT and GLe. The remaining articles were then separated into five categories based on the classification of IASP: 1) chronic widespread pain; 2) complex regional pain syndrome; 3) chronic primary headache or orofacial pain; 4) chronic primary visceral pain and 5) chronic primary musculosketal pain. If applicable, half of the articles in each category were separated and respectively analyzed by MS and PT. The remaining articles were analyzed by MM and GLe. Finally, each reviewer (MS, PT, MM

medRxiv preprint doi: https://doi.org/10.1101/2023.03.03.23286579; this version posted March 6, 2023. The copyright holder for this preprint (which was not certified by peer review) is the author/funder, who has granted medRxiv a license to display the preprint in perpetuity. It is made available under a CC-BY-ND 4.0 International license .

and GLe) extracted, based on the chart developed by PT, general study design information and dMRI-specific study data. An overview of the chart used by each reviewer is outlined in *table 1*.

Results

From the 370 unique articles initially identified, 247 articles remained after removing reviews and articles which did not fit our inclusion criteria for the title and abstract. Subsequent removal of: case-reports, articles not available in English and articles that only reported pain anecdotally yielded a total of 175 articles. Further exclusion of articles that did not acquire dMRI in brain regions or on a specified chronic pain condition population, left 107 articles. Then, the remaining articles were separated into three categories: chronic primary pain (62 articles), chronic secondary pain (41 articles) and articles missing information about the chronic pain condition (4 articles); only chronic primary pain articles were kept. Afterwards, we excluded articles where the dMRI was acquired: on a nerve, only on healthy participants and articles without results, leaving 58 articles. Additionally, one article was added at the end because it was mentioned several times by remaining articles, giving a total of 59 articles for the final analysis.

Chronic primary headache or orofacial pain

The IASP classification defines chronic primary headache or orofacial pain as headache or orofacial pain that occurs on at least 15 days per month for a period longer than 3 months. Daily pain duration is at least 2 hours (untreated) or may occur in several shorter attacks (29) .

This category yielded 21 articles from which: 11 studies were on migraine (31–41), two were on cluster headache (42,43) one on chronic headache (44), three on temporomandibular disorder (TMD) (45–47) and four on burning mouth syndrome (48–51)

For the migraine studies, four studies used TBSS to generate whole brain FA skeleton (31,37,39,40). Neeb et coll found no difference in FA, MD, AD, and RD between migraine

medRxiv preprint doi: https://doi.org/10.1101/2023.03.03.23286579; this version posted March 6, 2023. The copyright holder for this preprint (which was not certified by peer review) is the author/funder, who has granted medRxiv a license to display the preprint in perpetuity. It is made available under a CC-BY-ND 4.0 International license .

patients and HC. The other three studies further analyzed the TBSS results using tractography. Gomez-Beldarrain et coll., using a probabilistic white matter tract atlas, found lower FA in the right anterior insula, bilateral cingulate gyri and right uncinate fasciculus. Szabó et coll., using probabilistic tractography with a seeding in regions showing group differences from TBSS, found lower FA, higher MD and RD in the right frontal WM. Kattem Husøy et coll., using deterministic tractography with a whole brain seeding (FA > 0.25), studied patients with varying types of primary headaches, but only migraine and tension-type headache results were analyzed. They found higher AD in several areas of the skeleton, such as the CC and corticospinal tract (CST), in migraine and tension-type headaches groups. No differences were observed for FA, MD, and RD

Three studies have used TBSS to generate FA maps only (32,35,38). One study has mentioned using a linear model based (Basser and Pierpaoli, 1996) to generate FA maps (34). Zhang et coll, using SPM on diffusion metric maps registered to MNI, found no difference in FA, RD, and AD. Coppola et coll. have found notably higher RD in various WM tracts such as, the bilateral genu of the CC and the bilateral posterior limb of the IC. DaSilva et coll. have found lower FA in two regions of the brain in the posterior limb of the IC and the CR. Marciszewski et coll. have evaluated FA, AD, MD, and RD during different phases of the cycle of a migraine. Results showed variation of MD during the cycle of migraine in different regions such as the spinal trigeminal nucleus. Also, FA was higher in the region of the medial lemniscus/ventral trigeminal thalamic tract in the entire migraine cycle.

Three studies have used only tractography (33,36,41). Chong et coll. used TRACULA from Free Surfer to develop a classification model to distinguish migraine patients from persistent post-traumatic headache patients such that, no diffusion metrics were compared. Planchuelo-Gómez evaluated structural connectivity using the MRtrix tools. No diffusion metrics were compared, but they found an increase in streamline count in connections between subcortical regions, the insula, and the cingulate and orbitofrontal cortex and between the insula and the temporal region. Silvestro et coll. have used Bedpostx from FSL to investigate the brain connectome. No diffusion metrics were compared, but the connectome showed higher connection probability in precuneus, cuneus, amygdala, calcarine cortex, posterior cingulate cortex, anterior cingulate cortex, postcentral gyrus,

medRxiv preprint doi: https://doi.org/10.1101/2023.03.03.23286579; this version posted March 6, 2023. The copyright holder for this preprint (which was not certified by peer review) is the author/funder, who has granted medRxiv a license to display the preprint in perpetuity. It is made available under a CC-BY-ND 4.0 International license .

superior parietal lobule, lingual and fusiform gyri, middle frontal gyrus and inferior and superior parietal lobules.

For the cluster headache studies, both groups used TBSS to generate whole brain FA skeleton (42,43). Szabó et coll. reported diffusion metrics on the FA skeleton (FA, MD, AD, RD) and showed a decrease of FA in several WM tracts, such as the corpus callosum (CC) and the corona radiata (CR). While Teepker et coll. reported changes in FA in different structures, such as the internal capsule (IC) and thalamus, without specifying if they observed an increase or decrease of FA. Results from these two studies are therefore difficult to compare.

For the chronic headache study, the authors used constrained spherical deconvolution (CSD) and semi-automated tractography to compute whole brain tractograms, then extracted FA, RD and AD from two specific tracks, the cingulum and the uncinate fasciculus (44). FA and RD were respectively higher and lower in chronic headaches patients compared to healthy controls (HC) in the cingulum. No difference was observed in the uncinate fasciculus and for the AD metric on both bundles.

For the TMD studies, two studies used TBSS to generate whole brain FA skeleton and probabilistic tractography (45,46). Salomons et coll. evaluated the relation between FA of a corticospinal track and behavioral aspects, however, no comparison between groups regarding diffusion metrics was performed. In the other TBSS TMD study, Moayedi et coll. have showed lower FA notably in the right IC and the right external/extreme capsule adjacent to the insula. They also found, in the CC, higher connection probability to the frontal pole and lower connection probability to the dorsolateral prefrontal cortex. The authors did also dMRI on the trigeminal nerve directly, but those results were not included in this review.

Gustin et coll. have generated FA maps using classic Basser and Pierpaoli method (52) without referencing any specific software (47). FA was computed to determine whether the primary somatosensory cortex (S1) reorganization was associated with a change in regional anatomy in TMD and painful trigeminal neuralgia (PTN). They found that the S1 face

medRxiv preprint doi: https://doi.org/10.1101/2023.03.03.23286579; this version posted March 6, 2023. The copyright holder for this preprint (which was not certified by peer review) is the author/funder, who has granted medRxiv a license to display the preprint in perpetuity. It is made available under a CC-BY-ND 4.0 International license .

region FA was lower in the PTN compared to TMD and controls, but no difference was found between TMD and controls.

For the burning mouth syndrome studies, two articles have generated whole brain FA skeleton using TBSS (49,50) Khan et coll. also did probabilistic tractography.
In these two articles, no significant group differences in FA were found between patients suffering from burning mouth and controls. The remaining article used graph theoretical metrics to evaluate changes in the brain network at local and global connectivity using Brain Connectivity Toolbox (48,51). Wada et coll. showed higher connectivity at the bilateral rostral anterior cingulate cortex, right medial orbitofrontal cortex, and left pars orbitalis. Kurokawa et coll. showed higher betweenness centrality in the left insula, right amygdala, and right lateral orbito-frontal cortex and lower betweenness centrality in the right inferotemporal cortex. For both articles, no diffusion metrics were compared.

Chronic primary visceral pain

Chronic primary visceral pain is CPP localized in the head or neck, thoracic, abdominal, or pelvic region (29). The respective anatomical location is compatible with typical referral pain patterns from specific internal organs. Chronic primary visceral pain includes pain: in the head/neck viscera of the digestive system; in the thoracic region (e.g., noncardiac chest pain and reflux hypersensitivity); in the abdominal region arising from viscera of the digestive system (e.g., epigastric pain syndrome, irritable bowel syndrome, centrally mediated abdominal pain syndrome, and biliary dyskinesia) and in the pelvic region due to involvement of the viscera of the digestive, urinary, and genital systems (e.g., bladder pain syndrome, anal spasm, chronic pelvic pain, and chronic testicular pain).

For this category of pain, 19 studies were included. From these, seven studies focus only on irritable bowel syndrome (IBS) (53–59) (precisely, Nan et coll. focused on constipation-predominant IBS), three on only urological chronic pelvic pain syndrome (UCPPS) (60–62), four only on primary dysmenorrhea [PDM] (63–66), two on chronic prostatitis/ pelvic pain syndrome [CP/CPPS] (67,68), one on provoked vestibulodynia (PVD) (69), one on

medRxiv preprint doi: https://doi.org/10.1101/2023.03.03.23286579; this version posted March 6, 2023. The copyright holder for this preprint (which was not certified by peer review) is the author/funder, who has granted medRxiv a license to display the preprint in perpetuity. It is made available under a CC-BY-ND 4.0 International license .

interstitial cystitis/bladder pain syndrome (IC/BPS) (70) and one focused on two conditions: UCPSS and IBS (71).

Generally, all these papers have reported fractional anisotropy (FA) and mean diffusivity (MD) values. In studies with individuals suffering from IBS, the authors have, among other things, observed a higher FA value in posterior/anterior cingulate, corpus collosum, fornix and S1 regions when compared to control groups (53,54,56). However, the study of Hubbard and collaborators reported lower FA in the right dorsal cingulum bundle compared to controls and the study of Nan and collaborators reported lower FA in the corpus callosum (55,59). Although TBSS are used to extract metrics, the ROIs targeted are not the same between study. For example, a study looked at ROIs from white matter subserving areas associated with pain implicated in IBS including lateral (VPL) and medial (MD) thalamus, ACC (mid-anterior cingulum bundle), S1, insula and adjacent external capsule, and fornix (53) whereas another study focused on cingulum region essentially, from JHU atlas (55). Thus, the comparison between the different studies becomes difficult and hazardous.

For people with UCPPS, studies have shown that patients had lower FA and higher MD in brain regions commonly associated with perception and integration of pain information such as thalamus, basal ganglia and splenium of the corpus callosum (62,71). In contrast with the precedent studies, Huang and collaborators had observed that UCPPS patients exhibited higher FA in a portion of the left corticospinal track projecting through the precentral gyrus adjacent to the motor homunculus compared to control participants (61). Interestingly, a multi-site study has shown significant spatial variations in FA and the apparent diffusion coefficient (ADC, mathematically almost identical to MD) in statistical parametric maps for all healthy volunteers and UCPPS and positive control participants with adequate quality DTI when evaluated between sites (60). These observations thus highlight some of the consequences that multi-site studies can have for neuroimaging-based clinical phenotyping in UCPPS.

Moreover, compared to healthy controls, patients with PDM had increased FA along with decreased MD in the corpus callosum, superior longitudinal fasciculus, corona radiata,

medRxiv preprint doi: https://doi.org/10.1101/2023.03.03.23286579; this version posted March 6, 2023. The copyright holder for this preprint (which was not certified by peer review) is the author/funder, who has granted medRxiv a license to display the preprint in perpetuity. It is made available under a CC-BY-ND 4.0 International license .

internal and external capsule (66). While on the other hand, some studies have shown a lower FA in superior/posterior corona radiata, external capsule, dorsal-posterior cingulum and a higher MD in these same regions in patients with PDM (63,65). Also, another study has observed a significant negative correlation between the FA values of fiber tracks of thalamus-SI pathways and pain intensity in women with PDM, suggesting that women with higher level of pain had alteration in white matter integrity (64).

Chronic prostatitis/pelvic pain syndrome is another type of visceral pain. A study from Farmer and collaborators showed that there was no difference in mean whole brain white matter FA between patients with CP/CPPS and control participants (67). Using a different methodological approach, a DTI study used Trackvis diffusion toolkit to investigate the topological organization and proprieties of white matter brain network in patients with CP/CPPS (72). Briefly, the authors observed that the architecture of white matter networks of CP/CPPS patients and healthy controls were both presenting small-world properties. However, they showed that the frontal-parietal control network was presenting altered connectivity in patients with CP/CPPS.

Regarding the other subtype of visceral pain, individuals with PVD showed significant increases in the FA of the somatosensory and basal ganglia areas as well as a higher MD in the basal ganglia (internal capsule and pallidum) when compared to healthy controls (69). For IC/BPS patients, a study observed a decreased FA in parts of the right anterior thalamic radiation, left forceps major, and right longitudinal fasciculus, and an increased FA was detected in the right superior and bilateral inferior longitudinal fasciculi (70). Besides, these brain white matter abnormalities are correlated with symptom severity associated with IC/BPS.

Chronic primary musculoskeletal pain

Chronic primary musculoskeletal pain is CPP located in the muscles, bones, joints, or tendons (29). A typical example is chronic primary low-back pain. Chronic primary musculoskeletal pain syndromes are distinguished according to location: upper (chronic primary cervical pain), middle (chronic primary thoracic pain), lower back (chronic primary low-back pain), and limbs (chronic primary limb pain).

medRxiv preprint doi: https://doi.org/10.1101/2023.03.03.23286579; this version posted March 6, 2023. The copyright holder for this preprint (which was not certified by peer review) is the author/funder, who has granted medRxiv a license to display the preprint in perpetuity. It is made available under a CC-BY-ND 4.0 International license .

For this category of pain, ten studies were included. From these, five were on sub-acute/chronic low back pain (SBP/CLBP) (8,73–76), three on chronic musculoskeletal pain syndrome (77–79), one on nonspecific low back pain (80) and one on chronic neck pain (81).

For the low back pain studies, two were on a dataset that investigates transition from subacute to chronic low back pain (8,73). However, they used different methods that are not comparable, one used TBSS and identified clusters with lower FA only in subjects that transitioned to develop chronic pain (one cluster in the temporal part of left superior longitudinal fasciculus, a second located in the left retro-lenticular part of the internal capsule, and a third one in the left anterior limb of the internal capsule and part of the corpus callosum including the anterior corona radiata). While the other used probabilistic tractography to construct a network that identified a higher density of connections between corticolimbic regions (nucleus accumbens, amygdala, hippocampus-parahippocampus, and the prefrontal cortex) that were present in subjects that transitioned to develop chronic pain.

For the three studies specifically on chronic low back pain (75,76,82), one investigated WM regions on a TBSS skeleton that are adjacent to regions representing lower back and finger sensory regions as predetermined by fMRI experiments and were able to observe lower FA in those regions for the CLBP patients (76). Another study used the same concept, but for fMRI seeds located in the insula (75). They did not find differences in FA in the WM ROI bordering the insula between HC and CLBP, but they showed that FA of this region increased after spine surgery or facet joint block treatment in CLBP patients. The last study (82) also used TBSS to generate whole brain FA skeleton, but then segmented the skeleton using 50 WM ROIs from the ICBM-DTI-81 white matter atlas and found reduced FA in regions such as the corpus callosum, anterior and posterior thalamic radiation, SLF and corona radiata.

For chronic musculoskeletal pain syndrome, two studies are from the same group and most likely on an overlapping dataset comprising a heterogenous chronic pain population of ~ 50% of back pain, ~20 % of osteoarthritis (OA) and ~20% of post trauma patients. They either used TBSS only (78) or TBSS and a more complex multi-compartment Ball-and-

medRxiv preprint doi: https://doi.org/10.1101/2023.03.03.23286579; this version posted March 6, 2023. The copyright holder for this preprint (which was not certified by peer review) is the author/funder, who has granted medRxiv a license to display the preprint in perpetuity. It is made available under a CC-BY-ND 4.0 International license .

Sticks modeling (77) and found regional differences in the splenium of the corpus callosum (lower FA, mode of anisotropy [MO] and Ball-and-Sticks partial volume fraction metrics) and the cingulum (lower FA and partial volume fraction metric). They also reported changes in both DTI based (increases in RD and/or AD in these cases) and Ball-and-Sticks (decreases in MO and/or partial volume fraction) metrics in internal and external capsules, cerebral peduncles and SLF. The third study on chronic musculoskeletal pain syndrome is one of the only using a recent modeling of the diffusion signal with a Neurite Orientation Dispersion and Density Imaging (NODDI) approach (79). They observed lower WM orientation dispersion index in few regions such as the anterior corona radiata, the right posterior thalamic radiation, the uncinate fasciculus and the fornix.

The participants from the nonspecific low back pain study (80) could potentially be classified as CLBP as they cite comparable studies that included CLBP participants. Nonetheless, this study is the only one using graph theoretical metrics to evaluate changes in the white matter architecture of low back pain patients and cannot be compared to any others. They found that local efficiency, a network metric that characterizes the ability of a network node to process specialized information at the local level, was lower in the low back pain patients when compared to healthy controls.

The last MSK study is about chronic neck pain (81) and compared neck pain from traumatic and idiopathic origin to healthy controls in a women-only cohort. After generating FA and diffusivities maps, they used the ICBM-DTI-81 WM label atlas to extract properties of several ROIs, they found decreased FA, and increased MD and RD in the left cingulum hippocampus and tapetum in traumatic compared to idiopathic neck pain and in the left tapetum in traumatic neck pain patients compared to controls.

Chronic widespread pain

Chronic widespread pain is diffuse musculoskeletal pain in at least 4 of 5 body regions and in at least 3 or more body quadrants (as defined by upper–lower/left–right side of the body) and axial skeleton (neck, back, chest, and abdomen) (29,83). Chronic widespread pain is characterized by the core features of CPP, such as pain persisting for at least 3 months, and associated with significant emotional distress and/or functional disability.

medRxiv preprint doi: https://doi.org/10.1101/2023.03.03.23286579; this version posted March 6, 2023. The copyright holder for this preprint (which was not certified by peer review) is the author/funder, who has granted medRxiv a license to display the preprint in perpetuity. It is made available under a CC-BY-ND 4.0 International license .

For this category of pain, six studies were included. All of which were made on fibromyalgia (FM) patients (84–89). Some of the earliest publications were found in this subgroup (84,89), where they were using the lowest number of gradient directions (6 and 9) and basic diffusion maps obtained from unspecified software or possibly in house pipelines. These two studies found similar differences in the thalamus (lower FA), and the Lutz study also found higher FA in several other grey matter regions such as the postcentral gyri, amygdalae, and hippocampi. One study that investigated diffusion maps extracted from the GE MRI software FuncTool did not report any differences in their diffusion measure (88) and another one, that investigated probabilistic tractography with the FSL tools, found more connection within the cerebellum in FM patients when compared to controls (86). One study compared young and old FM patients and report a lower FA in the corpus callosum only in older patients using FSL TBSS approach (85). The last study used diffusion maps extracted from ExploreDTI software to investigate the effect of hyperbaric oxygen therapy in FM patients and found an increase in FA in anterior and superior thalamic radiation, left Insula and right thalamus following the therapy (87).

Complex regional pain syndrome (CRPS)

Complex regional pain syndrome (CRPS) is a type of CPP characterized by pain in a regional distribution that usually starts distally in an extremity after trauma and that is disproportionate in magnitude or duration to the typical course (of pain) after similar tissue trauma (29,90,91).

For this chronic pain condition, only two studies were found (92,93). Both studies used a whole brain TBSS approach. Hotta et coll. identified regions of the WM skeleton showing higher MD, AD and RD. They showed extensive clusters (between ~300 and 1400 voxels) in the corpus callosum, internal capsule, corona radiata and SLF, and smaller ones (between ~14 and 150 voxels) namely in the fornix, external capsule, posterior thalamic radiation and cingulum. As for Geha et coll., they showed lower FA in a cluster within the left callosal fiber track. In addition, they performed probabilistic tractography to trace and quantify pathways from these clusters in both groups. They observe that in the left hemisphere (ipsilateral to the seed), average number of connections at long distances (> 60

medRxiv preprint doi: https://doi.org/10.1101/2023.03.03.23286579; this version posted March 6, 2023. The copyright holder for this preprint (which was not certified by peer review) is the author/funder, who has granted medRxiv a license to display the preprint in perpetuity. It is made available under a CC-BY-ND 4.0 International license .

mm from seed), as well as total number of connections, were significantly lower in CRPS patients.

Discussion

The purpose of this review was to provide a critical summary of the use of brain dMRI for the study of primary chronic pain conditions. Each article was classified according to the latest IASP chronic pain definition, dMRI sequence and analysis method. The main findings of this review highlight the difficulty of delineating common white matter abnormalities for each chronic pain condition. This observation comes in part from the vast number of possibilities to analyze and further report results from dMRI data. Notably:

Twenty-three percent of studies (14/59) did not report diffusion metrics comparisons between CP and healthy controls (seven articles in the orofacial pain category, four articles in the visceral pain category, two articles in the musculoskeletal pain category and one article in the widespread pain category). Alternately, these articles used dMRI to develop prediction models, quantify graph theory properties, or correlated metrics with various behavioral and physiological parameters.
Fourteen percent of the studies (8/59) did not report any differences between the groups that were investigated. Of these, four were in the orofacial pain category (two migraine and two BMS studies), one in the musculoskeletal pain category (CLBP), two in the visceral pain category (one IBS and one CP/CPPS) and one on widespread pain (fibromyalgia).

Finally, six percent of the studies (4/59) reported differences of FA or ODI in the fornix (two in visceral pain, one in CRPS and one in MSK) even though, due to its unique location surrounded by CSF, it is most likely affected by partial volume effects (PVE) even when using state-of-the art dMRI acquisition sequences (94). Furthermore, as presented later, when using a TBSS approach, the fornix is almost absent from the TBSS FA skeleton.

Main critics of the approaches used in the 59 articles

medRxiv preprint doi: https://doi.org/10.1101/2023.03.03.23286579; this version posted March 6, 2023. The copyright holder for this preprint (which was not certified by peer review) is the author/funder, who has granted medRxiv a license to display the preprint in perpetuity. It is made available under a CC-BY-ND 4.0 International license .

Acquisition parameters

One of the main issues explaining the lack of dMRI reproducibility is the large variability of acquisition parameters. For example, a recent study reported "Multisite, multiscanner, and multisubject acquisitions for studying variability in diffusion weighted MRI " and showed that with certain acquisition parameters, interscanner (same subject) variability could approach intersubject (same scanner) variability (95). As for any MRI sequences, many parameters need to be properly chosen to ensure quality diffusion sensitized images. Three main parameters which drastically influence quality and analysis outcome are discussed. 1) the b value; representing the strength, duration and timing of the diffusion encoding gradients (96,97); 2) the number of diffusions encoding gradient directions; generally representing the number of diffusion gradient directions applied over a sphere (98,99); and 3) the voxel dimensions; representing the length, width and height of the 3D image voxels, (100). The most common sequences developed for dMRI, suggested for DTI had: a b value of 1000s/mm^2, 30 unique gradient directions and a 2mm isotropic resolution.

1) Across studies, the b-value parameter was the most stable with ~75% of studies using a b value of 1000. Still, some of the b-values reported were either in an unusual range (700, 800, 900, 1200 and 1300) without any explanation or were not even reported. A striking observation is that only two groups performed multi-shell acquisitions, an acquisition strategy which emerged over 15 years ago (101) that allows for state-of-the-art dMRI analysis and that with modern multiband sequences is easily doable in an acceptable amount of time (between 10 and 20 minutes at most).

2) When investigating the number of diffusions encoding gradient directions, we found that ~55% of the studies acquired a minimum of 30 directions (with a maximum of 99 directions). However, this parameter was also highly variable with some studies acquiring only six or nine directions, which is troublesome as the theoretical limit to properly describe a diffusion tensor is six gradient directions (102,103). In the context of tractography (and more generally fiber orientation estimation), high angular resolution diffusion imaging (HARDI) was introduced as an efficient acquisition strategy to overcome DTI limitations. Based on the acquisition of over 50 gradient directions at a single high b-

medRxiv preprint doi: https://doi.org/10.1101/2023.03.03.23286579; this version posted March 6, 2023. The copyright holder for this preprint (which was not certified by peer review) is the author/funder, who has granted medRxiv a license to display the preprint in perpetuity. It is made available under a CC-BY-ND 4.0 International license .

value, HARDI (paired with multi-shell acquisition) is also doable in an acceptable amount of time (between 10 and 20 minutes at most).

3) Lastly, when investigating image resolution, the overall voxel volume ranged from 2.4mm^3 to 20mm^3. Forty-seven percent of studies used the conventional 2mm isotropic resolution, however, substantial variation was also noted, with some studies acquiring highly anisotropic voxels (e.g. 1.875x1.873x3 or 2x2.5x4) which can bias dMRI analysis. For example, the bigger the voxel, the more likely the voxel will contain multiple fiber populations (i.e. decrease fiber orientation homogeneity) thus impacting diffusion metrics (100) and anisotropic voxels will impact tractography algorithm, especially in branching situation (104).

Overall, the observations made in this section highlight the need for more standardized acquisition parameters and pre-processing pipelines across chronic pain dMRI studies. In addition to DTI MRI sequence recommendations and following human connectome project (HCP) guidelines (105) we recommend that new studies acquire multi-shell HARDI data at over 2mm isotropic resolution and a b=0 reverse phase-encoded image to correct susceptibility image distortions. We think that recommending this type of acquisition scheme will leave most space for protocol evolution and optimization while promoting reproducibility and replicability across datasets and analysis methods. For a recent review of dMRI preprocessing, we refer to this article (106).

Processing and analysis tools

The tools provided by the FMRIB group at Oxford were the most used, with over 70% of the papers using one of the FSL tools to process their dMRI data. Almost 50% of the papers use the Tract Based Spatial Statistic (TBSS) pipeline (107) to identify voxel-wise differences. Although TBSS is a valid approach that provides significant advantages over classic whole-brain voxel-based analysis when it comes to group comparison, this method does not use the full potential of dMRI images as it summarizes the complexity of the whole-brain white matter to a few voxels wide WM skeleton. Furthermore, this approach does not completely exclude registration errors. Therefore, almost no information coming from tracks spanning up to the cortex or tracks that are smaller or located in complex

medRxiv preprint doi: https://doi.org/10.1101/2023.03.03.23286579; this version posted March 6, 2023. The copyright holder for this preprint (which was not certified by peer review) is the author/funder, who has granted medRxiv a license to display the preprint in perpetuity. It is made available under a CC-BY-ND 4.0 International license .

regions can be found in the TBSS maps. The other most commonly used softwares to process dMRI data were ExploreDTI (108) and MRtrix (109), both offering advanced tools specifically designed for dMRI data to generate tractography and diffusion metrics maps. To circumvent issues brought by TBSS, some studies presented here have used a clever approach to identify white matter tracts impacted by the chronic pain condition under study. They used the clusters of significant differences identified in the TBSS results as seeds to perform probabilistic tractography. Although this approach allows for the identification of actual white matter tracts that were not present in the WM skeleton, it still cannot reconcile the fact that a significant volume of white matter was not included in the original TBSS analysis. Similarly, several groups have identified GM ROI from fMRI experiments and then expanded this region to include adjacent white matter as a WM ROI to extract diffusion properties. However, this needs to be taken carefully as a WM bundle passing close to a GM region does not necessarily connect with that region. Indeed, many WM tracts travel long distances in the brain without connecting with each region they are bordering along the way. A more appropriate approach could have been to use the GM ROI to generate seeds from/to which WM fibers might connect and extract those tracks from a whole brain tractogram.

To illustrate the constraints of TBSS methods, we examined the disparities between TBSS and a track-based approach for two specific tracks, namely the fornix and the accumbofrontal (AcF) track, which are of particular significance in chronic pain research owing to the regions they connect. Notably, the fornix serves as the primary pathway for efferent signals from the hippocampus, and it plays a critical role in memory circuitry (94). Moreover, hippocampus volume has been shown to be a risk factor in the transition from acute to chronic pain (110). The AcF track connects the orbitofrontal cortex to the nucleus accumbens (111), both regions that are also implicated in the transition from acute to chronic pain (7). To demonstrate the benefits of employing targeted approaches for investigating white matter tracks involved in chronic pain, we analyzed the overlap of two streamline bundles extracted using separate techniques with a commonly used whole brain FA skeleton. For the first technique, data from a single subject from Mansour et coll. paper (73), that can be found on the OpenPain neuroimaging dataset platform (https://openpain.org) was used to generate a track segmentation of the left AcF track in

medRxiv preprint doi: https://doi.org/10.1101/2023.03.03.23286579; this version posted March 6, 2023. The copyright holder for this preprint (which was not certified by peer review) is the author/funder, who has granted medRxiv a license to display the preprint in perpetuity. It is made available under a CC-BY-ND 4.0 International license .

native imaging space. Firstly, the anatomical (T1w structural image, 1 mm isotropic) and diffusion data (8 b0s, 60 b1000, whole brain 2 mm isotropic) were processed using tractoflow version 2.3.0 (112) outputting a particle filtered whole brain tractogram (113). Next the brainnetome atlas was registered to the subject space using the T1w image and a non-linear registration using the ANTS toolbox (114) followed by a nearest neighbor interpolation of the Brainnetome atlas (115) to the diffusion data. Streamlines for the left AcF were segmented by selecting all streamlines that joined the brainnetome ROIs (left nucleus accumbens and the left orbital frontal gyrus). The AcF track was then registered to MNI space using the previously calculated non-linear transformation. For comparison of the FA skeleton to multiple methods, the population averaged right fornix used in the RecobundlesX analysis pipeline (116) along with the aforementioned left AcF track were overlaid on the binarized whole brain FA skeleton. As a quantitative measure of overlap, voxels intersected by these tracks were extracted and the percentage of voxels overlapping the binarized FA skeleton were output for each track. The fornix and AcF tracks are displayed in Figure 2 along with the percentage of overlapping voxels showing 15% voxels overlap between TBSS and tractography approached for the fornix (figure 2 left), and only 12% voxels overlap for the AcF track (figure 2 right). This analysis was reproduced for a few other subjects from the OpanPain database and similar overlaps were obtained (not shown).

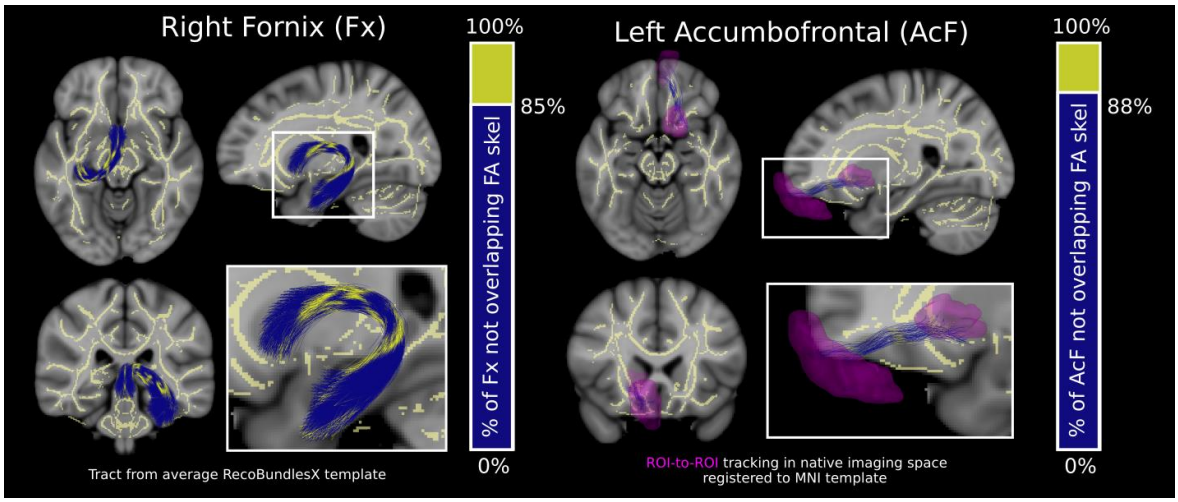

Figure 2. A visualization of the overlap between the FSL FA skeleton used commonly in whole brain diffusion MRI analysis and two different reconstructed white matter bundles taken from two different tractography analysis approaches. The population average right fornix (Fx) bundle used in the RecobundleX analysis pipeline is displayed in blue with

medRxiv preprint doi: https://doi.org/10.1101/2023.03.03.23286579; this version posted March 6, 2023. The copyright holder for this preprint (which was not certified by peer review) is the author/funder, who has granted medRxiv a license to display the preprint in perpetuity. It is made available under a CC-BY-ND 4.0 International license .

regions overlapping the FA skeleton displayed in yellow. Voxels overlapping the bundle were extracted and the percentage of these voxels overlapping the FA skeleton are displayed as a bar graph. The same metrics are displayed for the Left Accumbofronal (AcF) track which was generated in native imaging space by extracting tracks that traversed ROIs (pink) from the nucleus accumbens and the orbital frontal gyrus. Only a small proportion of these tracks overlap the whole brain FA skeleton from FSL, suggesting that more targeted analysis approaches may be more sensitive to detecting microstructural alterations in some white matter structures.

Where should the field go?

Similar to the challenge faced by fMRI for processing and analysis (103,104), dMRI is facing reproducibility and replication issues. For example, when observing results of this review, one is faced with the relatively large variation in published results, measures and methods across studies. Typically, three main parameters can be used to improve group comparisons and improve study replicability: i) Increasing group differences, ii) Increasing study sample size and, iii) decreasing intra-group variability.

i) Increasing group differences: To increase group differences, novel biomarkers that increase sensitivity and specificity must be found. Recent advances in MR hardware, acquisition schemes (HARDI, DSI, multi-shell) and analysis method allow the investigation of new brain markers (117). However, the CP field has yet to yield the full potential of these methods. A striking example is DTI. The DTI method has taken so much space in the field of dMRI of white matter that the two are often used interchangeably in literature. Furthermore, the latest studies about dMRI do not use DTI as it cannot accurately represent more than one fiber population per white matter voxel. Accordingly, the tensor model usually fails to capture proper microstructure in voxels where crossing fiber occurs and because this happens in about 60 to 90% of all white matter voxels in the brain (118) the DTI method is now seen as providing unanatomical sound information. There are several new methods that exists, each attempting to account for a better approximation of the underlying white matter tissue organization. Notably in the articles from this review, four studies used whole brain connectome metrics and two studies used multi-compartment local models.

medRxiv preprint doi: https://doi.org/10.1101/2023.03.03.23286579; this version posted March 6, 2023. The copyright holder for this preprint (which was not certified by peer review) is the author/funder, who has granted medRxiv a license to display the preprint in perpetuity. It is made available under a CC-BY-ND 4.0 International license .

ii) Increasing study sample size: Chronic pain lacks a large dMRI imaging open dataset. Recent improvements in metadata sharing, unthresholded statistical maps sharing, standardized dataset structures, multi-site harmonization, and standardized metrics could allow the rapid expansion of open-access datasets to study chronic pain.

iii) Decreasing intra-group variability: Both chronic pain and dMRI are subject to large intra-group variability. For chronic pain, intra-group variability can be mitigated by reducing chronic pain condition confounds (improving clinical evaluation specificity). Concerning dMRI, intra-group variability can be mitigated at each step of the study from acquisition to analysis. We would like to emphasize that, in the context of group comparisons, dMRI data presents additional challenges over other structural MR data such as region of interest positioning, registration and smoothing. Notably, due to these common dMRI pitfalls (119), application of commonly used structural MR analysis methods, such as whole brain voxel-based analysis, are discouraged. Therefore, we recommend that the acquisition parameters, pre-processing, processing and analysis be conducted with standardized pipelines specific to dMRI.

Overall, the goal of this review is not to favorize one over the other but to encourage the field to move towards more up to date modelling of dMRI signal and using methods along High Angular Resolution Diffusion Imaging (HARDI) concepts. This procedural update will allow pain researchers to capture subtle white matter abnormalities that cannot be observed with more conventional methods.

A note on acute pain

The link between white matter characteristics and acute pain perception, as often reported by pain thermal stimulation fMRI studies, is under-studied. Preliminary screening revealed that only 13 studies specifically investigated this aspect. Therefore, due to significant methodological differences compared to chronic pain, acute pain studies were excluded from this review.

Limitations

medRxiv preprint doi: https://doi.org/10.1101/2023.03.03.23286579; this version posted March 6, 2023. The copyright holder for this preprint (which was not certified by peer review) is the author/funder, who has granted medRxiv a license to display the preprint in perpetuity. It is made available under a CC-BY-ND 4.0 International license .

Due to evolving chronic pain defintions and dMRI nomenclature, it is likely that articles performing dMRI on primary chronic pain patients were missed in this review. For example, an article from Geha et al (93), referenced by other studies in this review, was erroneously excluded because its dMRI nomenclature did not meet our inclusion criteria. Moreover, the most recent chronic pain definition was used to select and classify the literature to be reviewed (29), therefore, some papers might have identified their participants otherwise would they have used these new definitions.

Author Approval

All authors have seen and approved the manuscript.

Conflits of interest

MD is co-founder of IMEKA inc.
All other authors declare no conflict of interest.

Funding

MS is supported by a PhD scholarship from the CIHR. GLi is supported by FRQS UNIQUE postdoctoral scholarship. PT is supported by FRQS J1 salary award and Arthritis Society star career development award. GLe is supported by FRQS J2 salary award.

medRxiv preprint doi: https://doi.org/10.1101/2023.03.03.23286579; this version posted March 6, 2023. The copyright holder for this preprint (which was not certified by peer review) is the author/funder, who has granted medRxiv a license to display the preprint in perpetuity. It is made available under a CC-BY-ND 4.0 International license .

References:

1. Baliki MN, Apkarian AV. Nociception, Pain, Negative Moods, and Behavior Selection. Neuron. 2015 Aug 5;87(3):474 491.
2. Kregel J, Meeus M, Malfliet A, Dolphens M, Danneels L, Nijs J, et al. Structural and functional brain abnormalities in chronic low back pain: A systematic review. Semin Arthritis Rheum. 2015 Oct;45(2):229–37.
3. Baliki MN, Schnitzer TJ, Bauer WR, Apkarian AV. Brain morphological signatures for chronic pain. PloS One. 2011;6(10):e26010.
4. Vachon-Presseau E, Tétreault P, Petre B, Huang L, Berger SE, Torbey S, et al. Corticolimbic anatomical characteristics predetermine risk for chronic pain. Brain J Neurol. 2016 Jul;139(Pt 7):1958–70.
5. Hashmi JA, Baliki MN, Huang L, Baria AT, Torbey S, Hermann KM, et al. Shape shifting pain: chronification of back pain shifts brain representation from nociceptive to emotional circuits. Brain J Neurol. 2013 Sep;136(Pt 9):2751 2768.
6. Baliki MN, Mansour AR, Baria AT, Apkarian AV. Functional Reorganization of the Default Mode Network across Chronic Pain Conditions. PloS One. 2014;9(9):e106133.
7. Baliki MN, Petre B, Torbey S, Herrmann KM, Huang L, Schnitzer TJ, et al. Corticostriatal functional connectivity predicts transition to chronic back pain. Nat Neurosci. 2012 Aug;15(8):1117–9.
8. Vachon-Presseau E, Tétreault P, Petre B, Huang L, Berger SE, Torbey S, et al. Corticolimbic anatomical characteristics predetermine risk for chronic pain. Brain J Neurol. 2016 Jul;139(Pt 7):1958–70.
9. Seminowicz DA, Wideman TH, Naso L, Hatami-Khoroushahi Z, Fallatah S, Ware MA, et al. Effective Treatment of Chronic Low Back Pain in Humans Reverses Abnormal Brain Anatomy and Function. J Neurosci Off J Soc Neurosci. 2011 May 18;31(20):7540 7550.
10. Tétreault P, Baliki MN, Baria AT, Bauer WR, Schnitzer TJ, Apkarian AV. Inferring distinct mechanisms in the absence of subjective differences: Placebo and centrally acting analgesic underlie unique brain adaptations. Hum Brain Mapp. 2018;3(5):e17.
11. Hutchinson EB, Schwerin SC, Avram AV, Juliano SL, Pierpaoli C. Diffusion MRI and the detection of alterations following traumatic brain injury. J Neurosci Res. 2018;96(4):612–25.
12. Andica C, Kamagata K, Hatano T, Saito Y, Ogaki K, Hattori N, et al. MR Biomarkers of Degenerative Brain Disorders Derived From Diffusion Imaging. J Magn Reson Imaging. 2020;52(6):1620–36.
13. Meijer FJA, Bloem BR, Mahlknecht P, Seppi K, Goraj B. Update on diffusion MRI in Parkinson's disease and atypical parkinsonism. J Neurol Sci. 2013;332(1–2):21–9.
14. Lakhani DA, Schilling KG, Xu J, Bagnato F. Advanced Multicompartment Diffusion MRI Models and Their Application in Multiple Sclerosis. Am J Neuroradiol. 2020;41(5):751–7.
15. Cabrera DV, Stobbe R, Smyth P, Giuliani F, Emery D, Beaulieu C. Diffusion tensor imaging tractography reveals altered fornix in all diagnostic subtypes of multiple sclerosis. Brain Behav. 2020;10(1):e01514.
16. Wang L, Leonards CO, Sterzer P, Ebinger M. White matter lesions and

medRxiv preprint doi: https://doi.org/10.1101/2023.03.03.23286579; this version posted March 6, 2023. The copyright holder for this preprint (which was not certified by peer review) is the author/funder, who has granted medRxiv a license to display the preprint in perpetuity. It is made available under a CC-BY-ND 4.0 International license .

depression: a systematic review and meta-analysis. J Psychiatr Res. 2014 Sep;56:56–64.
17. Tournier JD. Diffusion MRI in the brain – Theory and concepts. Prog Nucl Magn Reson Spectrosc. 2019;112:1–16.
18. Tracey I, Woolf CJ, Andrews NA. Composite Pain Biomarker Signatures for Objective Assessment and Effective Treatment. Neuron. 2019 Mar 6;101(5):783 800.
19. Reckziegel D, Vachon-Presseau E, Petre B, Schnitzer TJ, Baliki MN, Apkarian AV. Deconstructing biomarkers for chronic pain: context- and hypothesis-dependent biomarker types in relation to chronic pain. Pain. 2019 May;160 Suppl 1:S37 S48.
20. Mackey S, Greely HT, Martucci KT. Neuroimaging-based pain biomarkers: definitions, clinical and research applications, and evaluation frameworks to achieve personalized pain medicine. PAIN Rep. 2019;4(4):e762.
21. Miesen MM van der, Lindquist MA, Wager TD. Neuroimaging-based biomarkers for pain. PAIN Rep. 2019;4(4):e751.
22. Woo CW, Chang LJ, Lindquist MA, Wager TD. Building better biomarkers: brain models in translational neuroimaging. Nat Neurosci. 2017 Feb 23;20(3):365 377.
23. Mouraux A, Iannetti GD. The search for pain biomarkers in the human brain. Brain J Neurol. 2018 Nov 20;356(Pt 2):217.
24. Drake-Pérez M, Boto J, Fitsiori A, Lovblad K, Vargas MI. Clinical applications of diffusion weighted imaging in neuroradiology. Insights Imaging. 2018;9(4):535–47.
25. Tae WS, Ham BJ, Pyun SB, Kang SH, Kim BJ. Current Clinical Applications of Diffusion-Tensor Imaging in Neurological Disorders. J Clin Neurol. 2018;14(2):129–40.
26. Jespersen SN. White matter biomarkers from diffusion MRI. J Magn Reson. 2018;291:127–40.
27. Goveas J, O'Dwyer L, Mascalchi M, Cosottini M, Diciotti S, Santis SD, et al. Diffusion-MRI in neurodegenerative disorders. Magn Reson Imaging. 2015;33(7):853–76.
28. Kamagata K, Andica C, Kato A, Saito Y, Uchida W, Hatano T, et al. Diffusion Magnetic Resonance Imaging-Based Biomarkers for Neurodegenerative Diseases. Int J Mol Sci. 2021;22(10):5216.
29. Nicholas M, Vlaeyen JWS, Rief W, Barke A, Aziz Q, Benoliel R, et al. The IASP classification of chronic pain for ICD-11. PAIN. 2019;160(1):28–37.
30. Treede RD, Rief W, Barke A, Aziz Q, Bennett MI, Benoliel R, et al. Chronic pain as a symptom or a disease: the IASP Classification of Chronic Pain for the International Classification of Diseases (ICD-11). Pain. 2019 Jan;160(1):19–27.
31. Kattem Husøy A, Eikenes L, Håberg AK, Hagen K, Stovner LJ. Diffusion tensor imaging in middle-aged headache sufferers in the general population: a cross-sectional population-based imaging study in the Nord-Trøndelag health study (HUNT-MRI). J Headache Pain. 2019 Jul 10;20(1):78.
32. Zhang J, Wu YL, Su J, Yao Q, Wang M, Li GF, et al. Assessment of gray and white matter structural alterations in migraineurs without aura. J Headache Pain. 2017 Dec;18(1):74.
33. Chong CD, Berisha V, Ross K, Kahn M, Dumkrieger G, Schwedt TJ. Distinguishing persistent post-traumatic headache from migraine: Classification based on clinical symptoms and brain structural MRI data. Cephalalgia Int J Headache. 2021 Apr 29;333102421991819.
34. Marciszewski KK, Meylakh N, Di Pietro F, Macefield VG, Macey PM, Henderson LA. Fluctuating Regional Brainstem Diffusion Imaging Measures of Microstructure across the Migraine Cycle. eNeuro. 2019 Aug;6(4).

medRxiv preprint doi: https://doi.org/10.1101/2023.03.03.23286579; this version posted March 6, 2023. The copyright holder for this preprint (which was not certified by peer review) is the author/funder, who has granted medRxiv a license to display the preprint in perpetuity. It is made available under a CC-BY-ND 4.0 International license .

35. DaSilva AFM, Granziera C, Tuch DS, Snyder J, Vincent M, Hadjikhani N. Interictal alterations of the trigeminal somatosensory pathway and periaqueductal gray matter in migraine. Neuroreport. 2007 Mar 5;18(4):301–5.
36. Planchuelo-Gómez Á, García-Azorín D, Guerrero ÁL, Aja-Fernández S, Rodríguez M, de Luis-García R. Multimodal fusion analysis of structural connectivity and gray matter morphology in migraine. Hum Brain Mapp. 2021;42(4):908–21.
37. Neeb L, Bastian K, Villringer K, Gits HC, Israel H, Reuter U, et al. No microstructural white matter alterations in chronic and episodic migraineurs: a case-control diffusion tensor magnetic resonance imaging study. Headache. 2015 Feb;55(2):241–51.
38. Coppola G, Di Renzo A, Tinelli E, Petolicchio B, Di Lorenzo C, Parisi V, et al. Patients with chronic migraine without history of medication overuse are characterized by a peculiar white matter fiber bundle profile. J Headache Pain. 2020 Jul 18;21(1):92.
39. Gomez-Beldarrain M, Oroz I, Zapirain BG, Ruanova BF, Fernandez YG, Cabrera A, et al. Right fronto-insular white matter tracts link cognitive reserve and pain in migraine patients. J Headache Pain. 2015;17:4.
40. Szabó N, Kincses ZT, Párdutz Á, Tajti J, Szok D, Tuka B, et al. White matter microstructural alterations in migraine: a diffusion-weighted MRI study. Pain. 2012 Mar;153(3):651–6.
41. Silvestro M, Tessitore A, Caiazzo G, Scotto di Clemente F, Trojsi F, Cirillo M, et al. Disconnectome of the migraine brain: a “connectopathy” model. J Headache Pain. 2021 Aug 28;22(1):102.
42. Szabó N, Kincses ZT, Párdutz A, Tóth E, Szok D, Csete G, et al. White matter disintegration in cluster headache. J Headache Pain. 2013;14:64.
43. Teepker M, Menzler K, Belke M, Heverhagen JT, Voelker M, Mylius V, et al. Diffusion tensor imaging in episodic cluster headache. Headache. 2012 Feb;52(2):274–82.
44. Miller JV, Andre Q, Timmers I, Simons L, Rasic N, Lebel C, et al. Subclinical post-traumatic stress symptomology and brain structure in youth with chronic headaches. NeuroImage Clin. 2021 Mar 13;30:102627.
45. Salomons TV, Moayedi M, Weissman-Fogel I, Goldberg MB, Freeman BV, Tenenbaum HC, et al. Perceived helplessness is associated with individual differences in the central motor output system. Eur J Neurosci. 2012;35(9):1481–7.
46. Moayedi M, Weissman-Fogel I, Salomons TV, Crawley AP, Goldberg MB, Freeman BV, et al. White matter brain and trigeminal nerve abnormalities in temporomandibular disorder. Pain. 2012 Jul;153(7):1467–77.
47. Gustin SM, Peck CC, Cheney LB, Macey PM, Murray GM, Henderson LA. Pain and plasticity: is chronic pain always associated with somatosensory cortex activity and reorganization? J Neurosci Off J Soc Neurosci. 2012 Oct 24;32(43):14874–84.
48. Wada A, Shizukuishi T, Kikuta J, Yamada H, Watanabe Y, Imamura Y, et al. Altered structural connectivity of pain-related brain network in burning mouth syndrome-investigation by graph analysis of probabilistic tractography. Neuroradiology. 2017 May;59(5):525–32.
49. Khan SA, Keaser ML, Meiller TF, Seminowicz DA. Altered structure and function in the hippocampus and medial prefrontal cortex in patients with burning mouth syndrome. Pain. 2014 Aug;155(8):1472–80.
50. Tan Y, Wu X, Chen J, Kong L, Qian Z. Structural and Functional Connectivity Between the Amygdala and Orbital Frontal Cortex in Burning Mouth Syndrome: An

medRxiv preprint doi: https://doi.org/10.1101/2023.03.03.23286579; this version posted March 6, 2023. The copyright holder for this preprint (which was not certified by peer review) is the author/funder, who has granted medRxiv a license to display the preprint in perpetuity. It is made available under a CC-BY-ND 4.0 International license .

fMRI Study. Front Psychol. 2019;10:1700.
51. Kurokawa R, Kamiya K, Inui S, Kato S, Suzuki F, Amemiya S, et al. Structural connectivity changes in the cerebral pain matrix in burning mouth syndrome: a multi-shell, multi-tissue-constrained spherical deconvolution model analysis. Neuroradiology. 2021 Dec;63(12):2005–12.
52. Basser PJ, Pierpaoli C. Microstructural and physiological features of tissues elucidated by quantitative-diffusion-tensor MRI. J Magn Reson B. 1996 Jun;111(3):209–19.
53. Chen JYW, Blankstein U, Diamant NE, Davis KD. White matter abnormalities in irritable bowel syndrome and relation to individual factors. Brain Res. 2011 May 25;1392:121–31.
54. Ellingson BM, Mayer E, Harris RJ, Ashe-McNally C, Naliboff BD, Labus JS, et al. Diffusion tensor imaging detects microstructural reorganization in the brain associated with chronic irritable bowel syndrome. Pain. 2013 Sep;154(9):1528–41.
55. Hubbard CS, Becerra L, Heinz N, Ludwick A, Rasooly T, Yendiki A, et al. Microstructural White Matter Abnormalities in the Dorsal Cingulum of Adolescents with IBS. eNeuro. 2018 Aug;5(4).
56. Irimia A, Labus JS, Torgerson CM, Van Horn JD, Mayer EA. Altered viscerotopic cortical innervation in patients with irritable bowel syndrome. Neurogastroenterol Motil Off J Eur Gastrointest Motil Soc. 2015 Aug;27(8):1075–81.
57. Qi R, Liu C, Weng Y, Xu Q, Chen L, Wang F, et al. Disturbed Interhemispheric Functional Connectivity Rather than Structural Connectivity in Irritable Bowel Syndrome. Front Mol Neurosci. 2016;9:141.
58. Liu G, Li S, Chen N, Zhao Z, Guo M, Liu H, et al. Inter-hemispheric functional connections are more vulnerable to attack than structural connection in patients with irritable bowel syndrome. J Neurogastroenterol Motil. 2021;27(3):426–35.
59. Nan J, Zhang L, Chen Q, Zong N, Zhang P, Ji X, et al. White Matter Microstructural Similarity and Diversity of Functional Constipation and Constipation-predominant Irritable Bowel Syndrome. J Neurogastroenterol Motil. 2018 Jan 30;24(1):107–18.
60. Alger JR, Ellingson BM, Ashe-McNalley C, Woodworth DC, Labus JS, Farmer M, et al. Multisite, multimodal neuroimaging of chronic urological pelvic pain: Methodology of the MAPP Research Network. NeuroImage Clin. 2016;12:65–77.
61. Huang L, Kutch JJ, Ellingson BM, Martucci KT, Harris RE, Clauw DJ, et al. Brain white matter changes associated with urological chronic pelvic pain syndrome: multisite neuroimaging from a MAPP case-control study. Pain. 2016 Dec;157(12):2782–91.
62. Woodworth DC, Dagher A, Curatolo A, Sachdev M, Ashe-McNalley C, Naliboff BD, et al. Changes in brain white matter structure are associated with urine proteins in urologic chronic pelvic pain syndrome (UCPPS): A MAPP Network study. PloS One. 2018;13(12):e0206807.
63. Dun W, Yang J, Yang L, Ma S, Guo C, Zhang X, et al. Abnormal white matter integrity during pain-free periovulation is associated with pain intensity in primary dysmenorrhea. Brain Imaging Behav. 2017 Aug;11(4):1061–70.
64. He J, Dun W, Han F, Wang K, Yang J, Ma S, et al. Abnormal white matter microstructure along the thalamus fiber pathways in women with primary dysmenorrhea. Brain Imaging Behav [Internet]. 2020; Available from: https://www.scopus.com/inward/record.uri?eid=2-s2.0-

medRxiv preprint doi: https://doi.org/10.1101/2023.03.03.23286579; this version posted March 6, 2023. The copyright holder for this preprint (which was not certified by peer review) is the author/funder, who has granted medRxiv a license to display the preprint in perpetuity. It is made available under a CC-BY-ND 4.0 International license .

85092152388&doi=10.1007%2fs11682-020-00400-9&partnerID=40&md5=9e2830c5fd93a3c5a4609bee0bfa1781
65. Liu J, Liu H, Mu J, Xu Q, Chen T, Dun W, et al. Altered white matter microarchitecture in the cingulum bundle in women with primary dysmenorrhea: A tract-based analysis study. Hum Brain Mapp. 2017 Sep;38(9):4430–43.
66. Liu P, Wang G, Liu Y, Yu Q, Yang F, Jin L, et al. White matter microstructure alterations in primary dysmenorrhea assessed by diffusion tensor imaging. Sci Rep. 2016 May 10;6:25836.
67. Farmer MA, Chanda ML, Parks EL, Baliki MN, Apkarian AV, Schaeffer AJ. Brain functional and anatomical changes in chronic prostatitis/chronic pelvic pain syndrome. J Urol. 2011 Jul;186(1):117–24.
68. Huang X, Chen J, Liu S, Gong Q, Liu T, Lu C, et al. Impaired frontal-parietal control network in chronic prostatitis/chronic pelvic pain syndrome revealed by graph theoretical analysis: A DTI study. Eur J Neurosci. 2021 Feb;53(4):1060–71.
69. Gupta A, Woodworth DC, Ellingson BM, Rapkin AJ, Naliboff B, Kilpatrick LA, et al. Disease-Related Microstructural Differences in the Brain in Women With Provoked Vestibulodynia. J Pain. 2018 May;19(5):528.e1-528.e15.
70. Farmer MA, Huang L, Martucci K, Yang CC, Maravilla KR, Harris RE, et al. Brain White Matter Abnormalities in Female Interstitial Cystitis/Bladder Pain Syndrome: A MAPP Network Neuroimaging Study. J Urol. 2015 Jul;194(1):118–26.
71. Woodworth D, Mayer E, Leu K, Ashe-McNalley C, Naliboff BD, Labus JS, et al. Unique Microstructural Changes in the Brain Associated with Urological Chronic Pelvic Pain Syndrome (UCPPS) Revealed by Diffusion Tensor MRI, Super-Resolution Track Density Imaging, and Statistical Parameter Mapping: A MAPP Network Neuroimaging Study. PloS One. 2015;10(10):e0140250.
72. Huang X, Chen J, Liu S, Gong Q, Liu T, Lu C, et al. Impaired frontal-parietal control network in chronic prostatitis/chronic pelvic pain syndrome revealed by graph theoretical analysis: A DTI study. Eur J Neurosci. 2021 Feb;53(4):1060–71.
73. Mansour AR, Baliki MN, Huang L, Torbey S, Herrmann KM, Schnitzer TJ, et al. Brain white matter structural properties predict transition to chronic pain. Pain. 2013 Oct;154(10):2160–8.
74. Ma J, Wang X, Qiu Q, Zhan H, Wu W. Changes in Empathy in Patients With Chronic Low Back Pain: A Structural–Functional Magnetic Resonance Imaging Study. Front Hum Neurosci. 2020;14:326.
75. Ceko M, Shir Y, Ouellet JA, Ware MA, Stone LS, Seminowicz DA. Partial recovery of abnormal insula and dorsolateral prefrontal connectivity to cognitive networks in chronic low back pain after treatment. Hum Brain Mapp. 2015 Jun;36(6):2075 2092.
76. Kim H, Mawla I, Lee J, Gerber J, Walker K, Kim J, et al. Reduced tactile acuity in chronic low back pain is linked with structural neuroplasticity in primary somatosensory cortex and is modulated by acupuncture therapy. NeuroImage. 2020 Aug 15;217:116899.
77. Bishop JH, Shpaner M, Kubicki A, Clements S, Watts R, Naylor MR. Structural network differences in chronic muskuloskeletal pain: Beyond fractional anisotropy. NeuroImage. 2018 Nov 15;182:441–55.
78. Lieberman G, Shpaner M, Watts R, Andrews T, Filippi CG, Davis M, et al. White matter involvement in chronic musculoskeletal pain. J Pain. 2014 Nov;15(11):1110–9.
79. Cruz-Almeida Y, Coombes S, Febo M. Pain differences in neurite orientation

medRxiv preprint doi: https://doi.org/10.1101/2023.03.03.23286579; this version posted March 6, 2023. The copyright holder for this preprint (which was not certified by peer review) is the author/funder, who has granted medRxiv a license to display the preprint in perpetuity. It is made available under a CC-BY-ND 4.0 International license .

dispersion and density imaging measures among community-dwelling older adults. Exp Gerontol. 2021 Oct 15;154:111520.
80. Pijnenburg M, Hosseini SMH, Brumagne S, Janssens L, Goossens N, Caeyenberghs K. Structural Brain Connectivity and the Sit-to-Stand-to-Sit Performance in Individuals with Nonspecific Low Back Pain: A Diffusion Magnetic Resonance Imaging-Based Network Analysis. Brain Connect. 2016 Dec;6(10):795–803.
81. Coppieters I, De Pauw R, Caeyenberghs K, Lenoir D, DeBlaere K, Genbrugge E, et al. Differences in white matter structure and cortical thickness between patients with traumatic and idiopathic chronic neck pain: Associations with cognition and pain modulation? Hum Brain Mapp. 2018 Apr;39(4):1721–42.
82. Ma J, Wang X, Qiu Q, Zhan H, Wu W. Changes in Empathy in Patients With Chronic Low Back Pain: A Structural-Functional Magnetic Resonance Imaging Study. Front Hum Neurosci. 2020;14:326.
83. Butler S, Landmark T, Glette M, Borchgrevink P, Woodhouse A. Chronic widespread pain—the need for a standard definition. PAIN. 2016;157(3):541–3.
84. Sundgren PC, Petrou M, Harris RE, Fan X, Foerster B, Mehrotra N, et al. Diffusion-weighted and diffusion tensor imaging in fibromyalgia patients: a prospective study of whole brain diffusivity, apparent diffusion coefficient, and fraction anisotropy in different regions of the brain and correlation with symptom severity. Acad Radiol. 2007 Jul;14(7):839–46.
85. Ceko M, Bushnell MC, Fitzcharles MA, Schweinhardt P. Fibromyalgia interacts with age to change the brain. NeuroImage Clin. 2013;3:249–60.
86. Kim H, Kim J, Loggia ML, Cahalan C, Garcia RG, Vangel MG, et al. Fibromyalgia is characterized by altered frontal and cerebellar structural covariance brain networks. NeuroImage Clin. 2015;7:667–77.
87. Hadanny A, Bechor Y, Catalogna M, Daphna-Tekoah S, Sigal T, Cohenpour M, et al. Hyperbaric Oxygen Therapy Can Induce Neuroplasticity and Significant Clinical Improvement in Patients Suffering From Fibromyalgia With a History of Childhood Sexual Abuse-Randomized Controlled Trial. Front Psychol. 2018;9:2495.
88. Fayed N, Garcia-Campayo J, Magallón R, Andrés-Bergareche H, Luciano JV, Andres E, et al. Localized 1H-NMR spectroscopy in patients with fibromyalgia: a controlled study of changes in cerebral glutamate/glutamine, inositol, choline, and N-acetylaspartate. Arthritis Res Ther. 2010;12(4):R134.
89. Lutz J, Jäger L, de Quervain D, Krauseneck T, Padberg F, Wichnalek M, et al. White and gray matter abnormalities in the brain of patients with fibromyalgia: a diffusion-tensor and volumetric imaging study. Arthritis Rheum. 2008 Dec;58(12):3960–9.
90. Birklein F, Schlereth T. Complex regional pain syndrome—significant progress in understanding. PAIN. 2015;156(NA;):S94–103.
91. Bruehl S. Complex regional pain syndrome. BMJ. 2015;351:h2730.
92. Hotta J, Zhou G, Harno H, Forss N, Hari R. Complex regional pain syndrome: The matter of white matter? Brain Behav. 2017 May;7(5):e00647.
93. Geha PY, Baliki MN, Harden RN, Bauer WR, Parrish TB, Apkarian AV. The brain in chronic CRPS pain: abnormal gray-white matter interactions in emotional and autonomic regions. Neuron. 2008 Nov 26;60(4):570 581.
94. Cahn AJ, Little G, Beaulieu C, Tétreault P. Diffusion properties of the fornix assessed by deterministic tractography shows age, sex, volume, cognitive, hemispheric, and twin relationships in young adults from the Human Connectome Project. Brain Struct

medRxiv preprint doi: https://doi.org/10.1101/2023.03.03.23286579; this version posted March 6, 2023. The copyright holder for this preprint (which was not certified by peer review) is the author/funder, who has granted medRxiv a license to display the preprint in perpetuity. It is made available under a CC-BY-ND 4.0 International license .

Funct. 2021;1–15.
95. Cai LY, Yang Q, Kanakaraj P, Nath V, Newton AT, Edmonson HA, et al. MASiVar: Multisite, Multiscanner, and Multisubject Acquisitions for Studying Variability in Diffusion Weighted Magnetic Resonance Imaging. bioRxiv. 2021;2020.12.03.408567.
96. Stejskal EO, Tanner JE. Spin Diffusion Measurements: Spin Echoes in the Presence of a Time-Dependent Field Gradient. J Chem Phys. 1965;42(1):288–92.
97. Burdette JH, Durden DD, Elster AD, Yen YF. High b-Value Diffusion-Weighted MRI of Normal Brain. J Comput Assist Tomogr. 2001 Jul;25(4):515–9.
98. Lebel C, Gee M, Camicioli R, Wieler M, Martin W, Beaulieu C. Diffusion tensor imaging of white matter tract evolution over the lifespan. NeuroImage. 2012 Mar;60(1):340 352.
99. Ni H, Kavcic V, Zhu T, Ekholm S, Zhong J. Effects of number of diffusion gradient directions on derived diffusion tensor imaging indices in human brain. 2006;27(8):1776–81.
100. Oouchi H, Yamada K, Sakai K, Kizu O, Kubota T, Ito H, et al. Diffusion Anisotropy Measurement of Brain White Matter Is Affected by Voxel Size: Underestimation Occurs in Areas with Crossing Fibers. Am J Neuroradiol. 2007;28(6):1102–6.
101. Wu YC, Alexander AL. Hybrid diffusion imaging. NeuroImage. 2007 Jul 1;36(3):617–29.
102. Basser PJ, Mattiello J, Lebihan D. Estimation of the Effective Self-Diffusion Tensor from the NMR Spin Echo. J Magn Reson B. 1994;103(3):247–54.
103. Shrager RI, Basser PJ. Anisotropically weighted MRI. Magn Reson Med. 1998;40(1):160–5.
104. Neher P, Stieltjes B, Wolf I, Meinzer HP, Fritzsche KH. Analysis of tractography biases introduced by anisotropic voxels. In ISMRM Germany; 2013.
105. Glasser MF, Sotiropoulos SN, Wilson JA, Coalson TS, Fischl B, Andersson JL, et al. The minimal preprocessing pipelines for the Human Connectome Project. NeuroImage. 2013 Oct 15;80:105 124.
106. Tax CMW, Bastiani M, Veraart J, Garyfallidis E, Okan Irfanoglu M. What's new and what's next in diffusion MRI preprocessing. NeuroImage. 2022 Apr;249:118830.
107. Smith SM, Jenkinson M, Johansen-Berg H, Rueckert D, Nichols TE, Mackay CE, et al. Tract-based spatial statistics: voxelwise analysis of multi-subject diffusion data. NeuroImage. 2006 Jul 15;31(4):1487 1505.
108. Leemans A, Jeurissen B, Sijbers J, Jones DK. ExploreDTI: a graphical toolbox for processing, analyzing, and visualizing diffusion MR data. 2009;1.
109. Tournier JD, Smith R, Raffelt D, Tabbara R, Dhollander T, Pietsch M, et al. MRtrix3: A fast, flexible and open software framework for medical image processing and visualisation. NeuroImage. 2019;202:116137.
110. Vachon-Presseau E, Tétreault P, Petre B, Huang L, Berger SE, Torbey S, et al. Corticolimbic anatomical characteristics predetermine risk for chronic pain. Brain J Neurol. 2016 Jul;139(Pt 7):1958–70.
111. Karlsgodt KH, John M, Ikuta T, Rigoard P, Peters BD, Derosse P, et al. The accumbofrontal tract: Diffusion tensor imaging characterization and developmental change from childhood to adulthood. Hum Brain Mapp. 2015 Dec;36(12):4954–63.
112. Theaud G, Houde JC, Boré A, Rheault F, Morency F, Descoteaux M. TractoFlow: A robust, efficient and reproducible diffusion MRI pipeline leveraging Nextflow &

medRxiv preprint doi: https://doi.org/10.1101/2023.03.03.23286579; this version posted March 6, 2023. The copyright holder for this preprint (which was not certified by peer review) is the author/funder, who has granted medRxiv a license to display the preprint in perpetuity. It is made available under a CC-BY-ND 4.0 International license .

Singularity. NeuroImage. 2020;218:116889.
113. Girard G, Whittingstall K, Deriche R, Descoteaux M. Towards quantitative connectivity analysis: reducing tractography biases. NeuroImage. 2014 Sep;98:266–78.
114. Avants BB, Tustison NJ, Stauffer M, Song G, Wu B, Gee JC. The Insight ToolKit image registration framework. Front Neuroinformatics. 2014;8:44.
115. Fan L, Li H, Zhuo J, Zhang Y, Wang J, Chen L, et al. The Human Brainnetome Atlas: A New Brain Atlas Based on Connectional Architecture. Cereb Cortex. 2016;26(8):3508–26.
116. Garyfallidis E, Côté MA, Rheault F, Sidhu J, Hau J, Petit L, et al. Recognition of white matter bundles using local and global streamline-based registration and clustering. NeuroImage. 2018 Apr 15;170:283–95.
117. Assaf Y, Johansen-Berg H, Schotten MT de. The role of diffusion MRI in neuroscience. NMR Biomed. 2017;32(4):e3762.
118. Jeurissen B, Leemans A, Tournier J, Jones DK, Sijbers J. Investigating the prevalence of complex fiber configurations in white matter tissue with diffusion magnetic resonance imaging. Hum Brain Mapp. 2013;34(11):2747–66.
119. Jones DK, Cercignani M. Twenty-five pitfalls in the analysis of diffusion MRI data. Jens H Jensen JAH, editor. NMR Biomed. 2010 Aug;23(7):803 820.

Table 1

	Authors & year	Type of chronic pain	Sample characteristics size: main chronic pain/healthy controls & others type of chronic pain	dMRI sequence details (# of directions, b value (s/mm2, resolution))	Method used to extract metric	Main findings
Primary headache and orofacial pain (n=21)	Rattern Hosaj et al., 2019	Migraine	69/277	40 directions, b = 1000, 2×1×2.5 mm3	FA skeleton (FSL-TBSS) & Automated tractography (Camino package)	Higher RD in several areas, most prominent in CC, CST, IFOF, ILF and left SLF
	Zhang et al., 2017	Migraine	32/32	64 directions, b = 1000, 2×2×2 mm3	FA, RD and AD maps (FSL - DTIFIT)	No difference
	Chong et al., 2021	Migraine	34/0 & 48 patients with persistent post-traumatic headache	30 directions, b = 1000, 1.7 × 1.7 × 4 mm3	Probabilistic tractography (FreeSurfer - TRACULA)	DTI used to develop a classification model to distinguish individual migraine (no diffusion metrics compared)
	Marciszewski et al., 2019	Migraine	36/29	32 directions, b = 1000, 2x2x2.5 mm3	Diffusion maps (not specified)	Higher FA in the region of the medial lemniscus/ventral trigeminal thalamic tract
	DaSilva et al.,2007	Migraine	24/12	60 directions, b = 700, 2x2x2 mm3	Diffusion maps (Freesurfer & FSL - specific tools not specified)	Lower FA in the thalamocortical tract
	Planchuelo-Gómez et al., 2021	Migraine	110/50	61 directions, b = 1000, 2x2x2 mm3	Anatomically-constrained tractography (MRtrix tools)	Higher streamline count in connections between subcortical regions, the insula, and the cingulate and orbitofrontal cortex & between the insula and the temporal region
	Neeb et al., 2015	Migraine	42/21	67 directions, b = 1000, 2x2x2 mm3	FA skeleton (FSL-TBSS)	No difference
	Coppola et al., 2020	Migraine	37/18	30 directions, b = 1000, 2x2x2 mm3	FA skeleton (FSL-TBSS)	Higher RD in bilateral SCR and PCR, bilateral genu of the CC, bilateral posterior limb of IC, bilateral superior LF & higher MD in tracts of the right SCR and PCR, right superior LF, and right splenium of the CC
	Gomez-Beldarrain et al., 2015	Migraine	9/15	15 directions, b = 800, 1.75x1.75x2 mm3	FA skeleton (FSL-TBSS)	Lower FA in the right anterior insula, bilateral cingulate gyri and right uncinate fasciculus
	Szabó et al., 2012	Migraine	17/17	60 directions, b = 1000, 2.4x2.4x2.4 cm3	FA skeleton & probabilistic tractography (FSL - TBSS and FDT - not specified which tools of FDT)	Lower FA and Higher MD & PD in the centre of white matter fibre bundles (specially, in the right frontal white matter)
	Silvestro et al., 2021	Migraine	94/91	32 directions, b = 1000, 2.5x2.5x2.5 mm3	Probabilistic tractography (FSL - Bedpostx)	Connectogram of nodes and edges showed higher connection probability in precuneus, cuneus, amygdala, calcarine cortex, posterior cingulate cortex, anterior cingulate cortex, postcentral gyrus, superior parietal lobule, lingual and fusiform gyri, middle frontal gyrus and inferior and superior parietal lobules.
	Szabó et al., 2013	Cluster headache	13/16	60 directions, b = 1000, 2.4x2.4x2.4 cm3	FA skeleton (FSL-TBSS)	Lower FA in most of the major white matter pathways: the CC, bilaterally in the forceps minor and major, right corona radiata, left internal and external capsule, left cerebral peduncule, frontal portion of the left corona radiata, right parietal juxtacortical white matter, left inferior fronto-occipital fascicle
	Teepker et al., 2012	Cluster headache	7/7	30 directions, b = 1000, 2×2×2.4 mm3	FA skeleton (FSL-TBSS)	Changes of FA in the brain stem, the thalamus, the IC, the superior and inferior temporal region, the frontal lobe, the occipital lobe and the cerebellum.
	Miller et al., 2021	Chronic headache	30/30	32 directions, b = 800, 2.2x2.2x2.2 mm3	Constrained spherical deconvolution (Explore DTI) & semi-automated tractography (In-house software)	Higher FA and lower RD in the cingulum
	Salomons et al., 2012	TMD	17/19	23 directions, b = 1000, 1.875×1.875×3 mm3	FA skeleton + probabilistic tractography (FSL-TBSS & FDT - not specified which tools of FDT)	FA correlated to helplessness (no diffusion metrics compared)
	Moayedi et al., 2012	TMD	17/17	23 directions, b = 1000, 1.875×1.875×3 mm3	FA skeleton + probabilistic tractography (FSL-TBSS & FDT - not specified which tools of FDT)	Lower FA in anterior limb of the internal capsule (ICAL) and external/capsules (EC/ExC).
	Guolin et al., 2012	TMD	17/21	32 directions, b = 1000, 2x2x2.5 mm3	Diffusion maps (not specified)	DWI used to determine if the primary somatosensory cortex (S1) reorganization was associated with a change in regional anatomy (no diffusion metris compared)
	Wada et al., 2017	BMS	14/14	60 directions, b = 1000, 2.5x2.5x2.5 mm3	Graph theoretical network analysis (Brain connectivity Toolbox)	Local connectivity change in the anterior cingulate cortex (ACC) and prefrontal cortex (PFC) including the medial orbitofrontal cortex and pars orbitalis & Strengthened connection of the anterior cingulate cortex and medial prefrontal cortex with the basal ganglia, thalamus, and brain stem.
	Khan et al., 2014	BMS	9/9	64 directions, b = NA, 1.8x1.8x2 mm3	FA skeleton + probabilistic tractography (FSL-TBSS & not specified which tools in FSL)	No difference
	Tan et al., 2019	BMS	26/27	64 directions, b = 1000, 2× 2× 3 mm3	FA skeleton (FSL-TBSS)	No difference
	Kurokawa et al., 2021	BMS	14/11	47 directions, b = 1500 & 46 directions, b = 3000, 2x2x2 mm3	Graph theoretical network analysis (Brain connectivity Toolbox)	Higher betweenness centrality in the left insula, right amygdala, and right lateral orbito-frontal cortex & lower betweenness centrality in the right inferotemporal cortex. No difference in clustering coefficient, node degree, and small-wordness
Primary musculoskeletal pain (n=10)	Mansour et al., 2013	SBPr/SBPp/CLBP	23 SBPr; 23 SBPp; 24 CLBP/28	60 directions, b = 1000, 2x2x2 mm3	FA skeleton + probabilistic tractography (FSL-TBSS & FDT-PROBTRACKX)	Lower FA (one cluster in the temporal part of left superior longitudinal fasciculus, a second located in the left retro-lenticular part of the internal capsule, and a third one in the left anterior limb of the internal capsule and part of the corpus callosum including the anterior corona radiata) in SBPp
	Ma et al., 2020	CLBP	24/22	32 directions, b = 1000, 2x2x2 mm3	FA skeleton (FSL-TBSS)	Lower FA in the corpus callosum, anterior and posterior thalamic radiation, SLF and corona radiata.
	Vachon-Presseau et al., 2016	SBPr/SBPp/CLBP	39 SBPr; 30 SBPp; 23 CLBP/40	60 directions, b = 1000, 2x2x2 mm3	Probabilistic tractography (FSL - FDT- PROBTRACKX)	Higher density of connections between corticolimbic regions (nucleus accumbens, amygdala, hippocampus-parahippocampus, and the prefrontal cortex) in SBPp (no diffusion metrics compared)
	Ceko et al., 2015	CLBP	14/16	99 directions, b = 1000, 2x2x2 mm3	FA skeleton (FSL-TBSS)	No difference in FA in the WM ROI bordering the insula
	Kim et al., 2020	CLBP	102/50	30 directions, b= 1200 & 600, 2x2x2 mm3	FA skeleton (FSL-TBSS)	Lower FA in the S1-back region
	Pijnenburg et al., 2016	Non nonspecific CLBP	17/17	60 directions, b = 1300, 2.5x2.5x2.5 mm3	Constrained spherical deconvolution (CSD) & Graph theoretical network analysis (Brain Connectivity Toolbox)	Lower local efficiency lower (no diffusion metrics compared)
	Bishop et al., 2018	Chronic musculoskeletal pain	74/31	46 directions, b = 1200, 2x2x2 mm3	FA skeleton + complex multi-compartment Ball-and-Sticks modeling (FSL-TBSS & FSL-FDT-Bedpostx)	Lower FA, MO and Ball-and-Sticks partial volume fraction metrics in the splenium of the corpus callosum and the cingulum
	Lieberman et al., 2014	Chronic musculoskeletal pain	46/33	46 directions, b = 1200, 2x2x2 mm3	FA skeleton (FSL-TBSS)	Lower FA in the splenium of corpus callosum, and left cingulum & higher RD in the splenium, right anterior and posterior limbs of internal capsule, external capsule, superior longitudinal fasciculus, and cerebral peduncle & higher AD bilaterally in the anterior limbs of internal capsule, and in the right cerebral peduncle.
	Cruz-Almeida et al., 2021	Chronic musculoskeletal pain	28/18	70 directions , b = 100 & b = 1000, 2x2x2 mm3	NODDI (AMICO)	Lower WM orientation dispersion index (ODI) in the Anterior Corona Radiata, right Posterior Thalamic Radiation, uncinate Fasciculus, superior Cerebellar Peduncle and the Fornix
	Coppieters et al., 2018	Chronic neck pain	74/31	64 directions, b = 1200, 2.5x2.5x2.5 mm3	Diffusion maps (Explore DTI)	Lower FA, and higher MD & RD in the left cingulum hippocampus and tapetum
Primary visceral pain (n=19)	Dun et al., 2017	PDM	24/24	60 directions, b = 1000, 2x2x2 mm3	FA skeleton (FSL-TBSS)	Lower FA, higher MD & RD in widespread WM fibers including the splenium part of the corpus callosum, the posterior limb of the internal capsules, the anterior, superior and posterior corona radiata, and the posterior thalamic radiation
	He et al., 2020	PDM	47/47	30 directions, b = 1000, 2x2x2 mm3	Automated TABS (not specified)	Lower FA in the thalamus-SI and thalamus-insula, and higher FA in the thalamus-dACC/SMA and thalamus-ACC
	Liu et al., 2017	PDM	41/41	30 directions, b = 1000, 2x2x2 mm3	FSL skeleton + Automated TABS (FSL-TBSS & not specified which tools in FSL)	Lower FA in the superior and posterior part of the corona radiata (white matter mainly located in the dorsal part of the cingulum bundle (lower FA & AD, higher MD) & parahippocampal sections of the cingulum bundle (lower FA & RD, higher MD)
	Liu et al., 2016	PDM	35/35	30 directions, b = 1000, 1.875×1.875x3 mm3	FA skeleton (FSL-TBSS)	Higher FA mainly in tracts of the CC (genu, body and splenium), fornix, bilateral IC, bilateral EC, CR, bilateral posterior TR, bilateral sagittal stratum, right cingulum and bilateral superior LF.
	Irimia et al., 2015	IBS	66/23	68 directions, b=NA, 2x2x2 mm3	Diffusion maps (not specified) + tractography (TrackVis)	Higher FA in S1
	Ellingson et al., 2013	IBS	33/93	64 directions, b=1000, 3x3x3 mm3 & 61 directions, b = 1000, 2.25x2.25x2 mm3	Diffusion maps & probabilistic tractography (AFNI/FSL - not specified which tools & FSL - FDT - Bedpostx)	Lower FA in thalamic regions, the basal ganglia and sensory/motor association/integration regions, frontal lobe regions and the corpus callosum and lower MD, within the globus pallidus, and higher MD in the thalamus, IC, and CR projecting to sensory/motor regions.
	Qi et al., 2016	IBS	65/67	20 directions, b = 1000, 1.8×1.8× 4 mm3	Tractography (TrackVis)	Higher interhemispheric FC between bilateral thalami, cuneus, posterior cingulate cortices (PCC), lingual gyri and inferior occipital/cerebellum lobes, as well as lower interhemispheric FC between bilateral ventral anterior cingulate cortices (vACC) and inferior parietal lobules (IPL) (no diffusion metrics compared).
	Hubbard et al., 2018	IBS	16/16	64 directions, b = 1000, 2x2x2 mm3	FA skeleton + probabilistic tractography (FSL-TBSS & not specified which tools in FSL)	Lower FA in the right dorsal cingulum bundle
	Chen et al., 2011	IBS	10/16	23 directions, b = 1000, 1.875×1.875×3 mm3	FA skeleton (FSL-TBSS)	Higher FA in the fornix and external capsule
	Nan et al., 2018	IBS	20/19	30 directions, b = 1000, 1.875×1.875×3 mm3	FA skeleton (FSL-TBSS)	Lower FA in the genu of the CC
	Liu et al., 2021	IBS	34/33	NA directions, b= NA, 2×2×3 mm3	Diffusion maps + Tractography	No difference (fiber length, and fiber number)
	Woodworth et al., 2015	UCPP & IBS	45 UCPP; 39 IBS/56	60-64 directions (multiple sites), b = 1000, 2x2x2 mm3	Diffusion maps (MRtrix tools)	Lower FA in UCPPS in the genu and splenium of the CC & a higher MD in the basal ganglia, association fibers and right superior and posterior CR fibers, CR fibers on the left hemisphere, and areas within the genu of the CC
	Huang et al., 2016	UCPP	19/32	60-69 directions (multiple sites), b = 1000, 2x2x2 mm3 & 0.85×0.85× 2 mm3	FA skeleton (FSL-TBSS)	Lower FA in the anterior thalamic radiation
	Woodworth et al., 2018	UCPP	30/0	60 directions & 61 directions (multiple sites), b = 1000, 2x2x2 mm3	Diffusion maps (Mrtrix tools)	DTI used to evaluation the correlation between DTI measurements and urinary protein quantification (no diffusion metrics compared)
	Alger et al., 2016	UCPP	98/128	33-64 directions (multiple sites), b =1000, 2x2x2 mm3 & 1.6x1.6x4 mm3 & 1.6x1.6x2 mm3	Diffusion maps (Mrtrix tools)	Main of the study was to evaluate variability in FA measurements obtained in other sites (no diffusion metrics compared)
	Farmer et al., 2011	CP/CPPS	19/16	60 directions, b = 1000, 1.7×1.7×2 mm3	FA skeleton (FSL-TBSS) + probabilistic tractography	No difference
	Huang et al., 2021	CP/CPPS	19/32	30 directions, b = 1000, 1.875×1.875×3 mm3	Tractography (TrackVis) + graph theoretical network analysis (In-house software)	Lower global efficiency in the right middle frontal gyrus (orbital part) and higher global efficiency in the left middle cingulate and paracingulate gyri (no diffusion metrics compared)
	Farmer et al., 2015	IC/BPS	44/44	60 directions (multiple sites), b=1000, 1.7×1.7×2 mm3 and 2x2x2 mm3	FA skeleton + probabilistic tractography (FSL-TBSS & FSL-FDT-not specified which tools in FDT)	Lower FA in aspects of the right anterior thalamic radiation, left forceps major, and right longitudinal fasciculus & Increased FA in the right superior and bilateral inferior longitudinal fasciculi.
	Gupta et al., 2018	PVD	28/29	60 directions & 64 directions, b = 1000, 2x2x2mm3	Diffusion maps (ANTM)	Higher FA in somatosensory and basal ganglia regions compared to PVD (higher MD in the basal ganglia (in the internal capsule and putamen) compared to PVD)
Chronic whidespread pain (n=6)	Sundgren et al., 2007	Fibromyalgia	19/25	9 directions, b = 1000, 2x2.5x4 mm3	Diffusion maps (not specified)	Lower FA in the right thalamus
	Ceko et al., 2013	Fibromyalgia	22/32	99 directions, b = 1000, 2x2x2 mm3	FA skeleton + probabilistic tractography (FSL-TBSS & FSL-FDT-not specified which tools in FDT)	Lower FA in the corpus callosum (older FM) & no difference for young FM
	Kim et al., 2015	Fibromyalgia	30/39	60 directions, b = 700, 2x2x2 mm3	Probabilistic tractography (FSL - FDT - BedpostX)	More connections within the cerebellum (no diffusion metrics compared)
	Hadanny et al., 2018	Fibromyalgia	30/0	30 directions, b = 1000, 1.5x1.5x2.2 mm3	Diffusion maps (Explore DTI)	Higher FA in anterior thalamic radiation, left Insula and right thalamus and superior thalamic radiation
	Fayed et al., 2010	Fibromyalgia	10/10	25 directions, b = 1000, 1.875x1.875x3 cm3	Diffusion maps (Functool software)	No difference
	Lutz et al. 2008	Fibromyalgia	30/30	6 directions, b = 1000, 1.8 x1.8x3.6 mm3	Diffusion maps (not specified)	Lower FA in Both thalami, the thalamocortical tracts, and both insular regions & higher FA in the postcentral gyri, amygdalae, hippocampi, superior frontal gyri, and anterior cingulate gyri.
Complex regional pain syndrome (n=2)	Hotta et al., 2017	CRPS	12/12	60 & 64 directions, b=1000, 1.875×1.875×3 mm3	FA skeleton (FSL-TBSS)	Higher MD, AD & RD in the genu, body, and splenium of corpus callosum, as well as in the left anterior and posterior and the right superior parts of the corona radiata.
	Gupta et al. 2009	CRPS	21/21	60 directions, b=1000, 1.7×1.7×2 mm3 and 2x2x2 mm3	FA skeleton & probabilistic tractography (FSL - TBSS and FDT - not specified which tools of FDT)	Lower FA values in a cluster within the left callosal fiber tract